Geotech Geol Eng
https://doi.org/10.1007/s10706-024-02878-2

ORIGINAL PAPER

Design and Installation of a Local Monitoring System to Validate Debris Flow Methodology for Risk Mitigation

Nicola Moraci · Mariantonietta Ciurleo · Maria Clorinda Mandaglio · Marilene Pisano

Received: 20 May 2024 / Accepted: 18 July 2024

Abstract Landslides pose significant threats to communities and infrastructure worldwide, necessitating the development of effective hazard and exposure reduction strategies to mitigate the potential risks. In particular, debris flows can be highly destructive landslides. The paper deals with an integrated monitoring system designed both to further validate an existing debris flow inception and propagation methodology developed by the authors and to fine-tune the landslide inception and warning model to be used in an early warning system. The design of the integrated monitoring system, the definition of the acquisition time of instruments, and the processing of the measured data were based on studies performed in the study area of Favazzina (Italy), which is affected by debris flows that are very difficult to monitor. The proposed approach used to design the integrated monitoring system may serve as a useful methodological tool to be adopted in similar geological and geotechnical contexts within the framework of risk mitigation strategies.

Keywords Integrated monitoring system · Instrumentation · Rapid landslide · Risk mitigation · Early warning systems

N. Moraci (✉) · M. Pisano
Department of Civil, Energy, Environmental and Materials Engineering, Mediterranea University of Reggio Calabria, Via R. Zehender, Località Feo di Vito, 89122 Reggio Calabria, Italy
e-mail: nicola.moraci@unirc.it

M. Pisano
e-mail: marilene.pisano@unirc.it

M. Ciurleo
National Research Council of Italy, Research Institute for Geo-Hydrological Protection (CNR - IRPI), Via Cavour 4-6, 87036 Rende, CS, Italy
e-mail: mariantonietta.ciurleo@irpi.cnr.it

M. C. Mandaglio
Department of Civil Engineering, University of Salerno, Via Giovanni Paolo II, 84084 Fisciano, SA, Italy
e-mail: mmandaglio@unisa.it

1 Introduction

Debris flows, triggered by various factors such as heavy rainfall, seismic activity or human-induced changes, can have devastating consequences on exposed elements such as people, structures, infrastructure, environmental assets, and architectural heritage. Analysing debris flow risk requires evaluating susceptibility, hazard zoning, and the scenario consequences of the events on the exposed elements. According to the quantitative risk approach (Fell et al. 2005, 2008; Corominas et al. 2014), three different mitigation strategies may be adopted to reduce landslide risk: (i) hazard reduction strategies, i.e. measures that decrease the likelihood of landslide occurrence or the probability of a landslide reaching the most exposed element; (ii) exposure reduction strategies, i.e. measures that

Published online: 01 August 2024

reduce the probability of elements being within the affected area during a landslide event at the time of its occurrence; (iii) vulnerability reduction strategies, i.e. measures that mitigate the potential loss or damage of elements exposed at risk (Guidelines AGI-ISPRA 2022).

Among hazard reduction strategies, prevention and protection measures may be used to reduce the inception occurrence of a landslide of fixed magnitude, as well as the probability that it reaches the elements at risk. Specifically, prevention measures can modify the balance between actions and resistances along the failure surface, transfer stable forces from stable zones to potentially unstable ones, increase the available shear strength, and prevent erosion and infiltration caused by rainfall; protection measures can control the direction of the landslide or dissipate its kinetic energy.

Among exposure reduction strategies, monitoring, alert systems and emergency plans, which identify and manage the paroxysmal phases of landslides by alerting and/or temporarily relocating the population, are increasingly adopted worldwide also due to cost-effectiveness. According to Calvello (2017) and Pecoraro et al. (2019), a key component of an early warning system for weather-induced landslides is the landslide model, which links weather data and landslide events by considering monitoring data and the geological, geomorphological, hydrogeological and geotechnical characteristics of the area of interest.

Previous studies by the authors (Ciurleo et al. 2019, 2020, 2021, 2022; Gioffrè et al. 2023; Moraci et al. 2017, 2024) developed an integrated methodology for analysing debris flow inception, propagation and accumulation, as well as its possible effects on exposed elements. The proposed methodology uses a dynamic and upgradable database with site-specific soil mechanical and hydraulic properties, geological data, soil cover thickness, topography and rheological data obtained from field and laboratory investigations. TRIGRS ("Transient Rainfall Infiltration and Grid-Based Regional Slope-Stability", Baum et al. 2002) predicts shallow landslide source areas of debris flows (inception analysis), while GeoFloW-SPH ("Smoothed Particle Hydrodynamics", Pastor et al. 2009) simulates propagation and deposition stages. This methodology proved to be robust, efficient and reliable in modelling debris flows occurred in the Favazzina study area (Italy).

Aligned with the quantitative risk approach (Fell et al. 2005, 2008; Corominas et al. 2014), the proposed methodology serves as a useful tool for the design of possible hazard and exposure reduction strategies.

This paper introduces an integrated monitoring system designed both to validate further the previously described debris flow inception and propagation methodology and to develop a warning model to be used in an early warning system. The integrated monitoring system was implemented in the Favazzina study area, where the proposed methodology was applied to model past debris flow events.

2 Favazzina Study Area

The study area is located within the "Costa Viola" between Scilla and Bagnara Calabra municipalities (Calabria, Italy) in the South-West Italy. The extension of the study area, which is periodically affected by debris flows, is about 1 km^2 (Fig. 1). The first historical report of debris flow occurrence in the area dates back to 1894 when a debris flow affected the railway line located in the coastal plain. The most significant debris flows, in terms of consequences, occurred on 12 May 2001, and 31 March 2005. The propagation paths of these events hit the SNAM methane pipeline, the State Road 18, the hamlet of Favazzina and the railways, causing the derailment of two trains. The 2001 debris flow was characterized by two triggering volumes that merged in the middle portion of the slope, while the 2005 debris flow was characterized by three triggering volumes. In both cases, the debris flows exhibited high velocity andstrong entrainment of material and water from the flow path.

The geological units of the area consist of a high-grade metamorphic rock basement from the Paleozoic era, which is strongly tectonized and deeply weathered, and is locally covered by sedimentary deposits from the Upper Pliocene to the Holocene.

From bottom to top, the weathering sequence of the Paleozoic basement includes moderately weathered rocks (class III gneiss), which rarely crop out, highly weathered rocks (class IV gneiss), which outcrop in the mid to lower portions of the slopes, completely weathered or saprolite rocks (class V gneiss), prevailing in the uppermost parts of the slopes, and

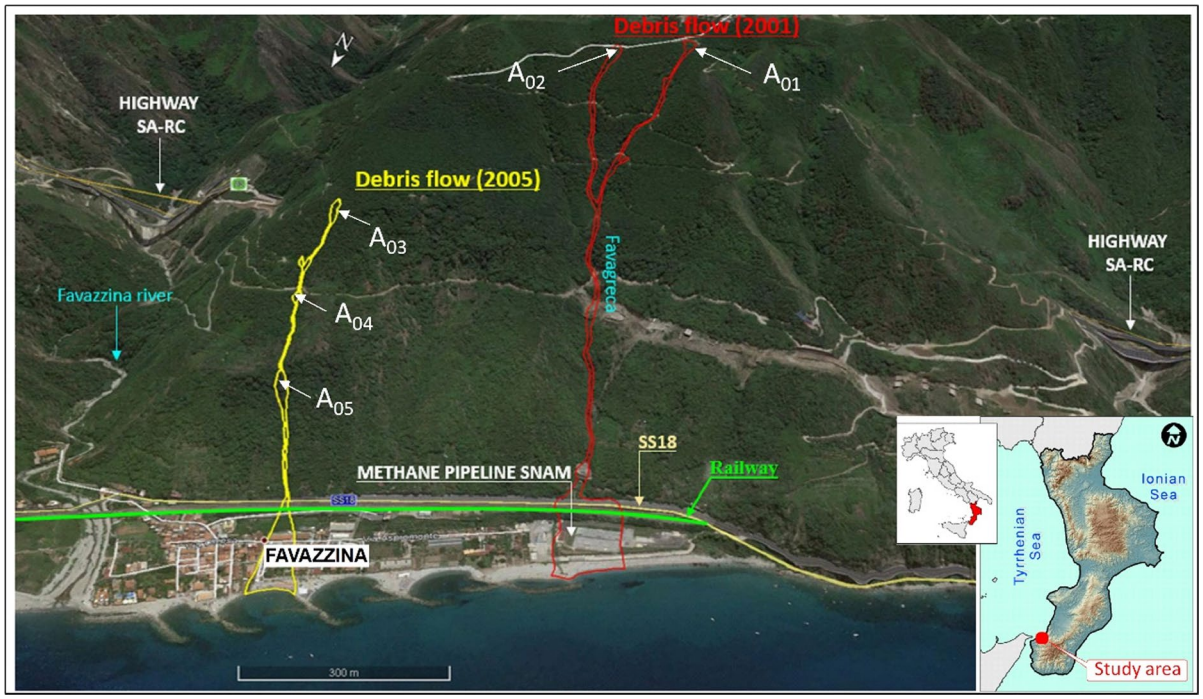

Fig. 1 Location of the Favazzina study area (modified from Ciurleo et al. 2021). A_{01} and A_{02} are the 2001 debris flow triggering areas; A_{03}, A_{04} and A_{05} are the 2005 debris flow triggering areas

residual, colluvial and detrital soils (class VI gneiss), which cover about 60% of the study area (Fig. 2).

An extensive on-site survey campaign and several sampling activities were performed in sites identified as most susceptible to debris flow occurrence (Ciurleo et al. 2021). Geotechnical laboratory tests were carried out on specimens retrieved from undisturbed samples taken on site to characterize the residual, colluvial and detrital soils (class VI gneiss) involved in the debris flows. Mineralogical classification of these soils (samples taken at depths ranging from 0.5 to 1.0 m) revealed the presence of quartz, feldspars (albite and microcline), phyllosilicates (biotite), and kaolinite, highlighting the typical composition of weathered gneiss (Biondino et al. 2020).

The on-site survey campaign, carried out through continuous mechanical borehole drillings and seismic refraction tomographies, identified the thickness of class VI gneiss, which is generally less than 2 m at the heads of the slopes where the debris flow triggering may occur.

According to the Unified Soil Classification System (USCS), residual, colluvial and detrital soils (class VI gneiss) can be classified as silty sand (SM)

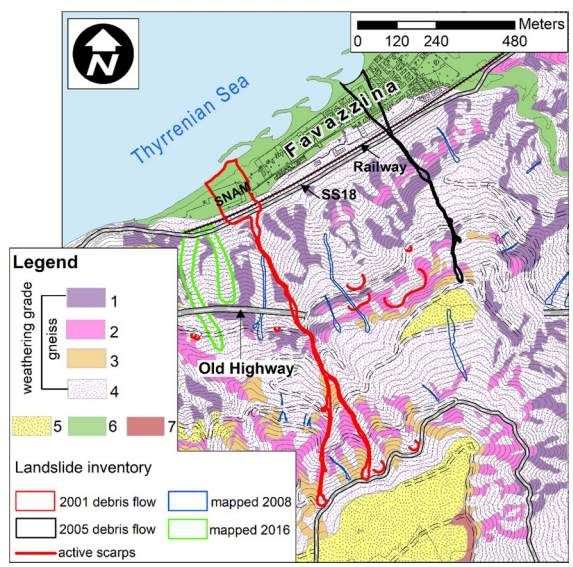

Fig. 2 Weathering grade map with geomorphological characteristics and multi-temporal landslide inventory. Legend: (1) weathered gneiss of class III; (2) weathered gneiss of class IV; (3) weathered gneiss of class V; (4) weathered gneiss of class VI; (5) terraced marine deposits; (6) coastal and alluvial deposits; (7) sandstone (modified from Ciurleo et al. 2022)

and clayey sand (SC) with an inorganic fine fraction of medium compressibility and no activity. The liquid limit (LL) and plasticity index (PI) range from 30.2 to 33.4% and from 3.2 to 11.4%, respectively. The solids unit weight (γ_s) varies from 25.9 to 26.1 kN/m^3, the void ratio (e) ranges from 0.90 to 1.17, and the soil porosity (n) varies from 0.40 to 0.55.

Triaxial compression tests on saturated undisturbed specimens of residual soils (class VI gneiss) showed a hardening behaviour. The peak shear strength parameters, i.e. effective cohesion (c′) and effective shear strength angle (ϕ′), range from 0 to 5 kPa and from 30° to 40°, respectively. The saturated hydraulic conductivity (K_{sat}) and the saturated volumetric water content (θ_s) range from 1.84 E−08 m/s to 3.64 E−07 m/s and from 0.38 to 0.40, respectively.

3 Integrated Monitoring System

An integrated monitoring system can serve different purposes. When the goal is to improve the understanding of landslide processes, it comprises a network of instruments capable of collecting essential field measurements to enhance knowledge of landslide models, as well as to calibrate and validate numerical models used for landslide simulation.

For integrated monitoring systems used as part of landslide early warning systems (LEWSs), they include tools and technologies necessary not only to monitor the landslide phenomena but also to generate and disseminate timely and meaningful warning information to individuals, communities and organizations threatened by a hazard. This enables them to take appropriate actions in time to reduce the possibility of harm or loss of human life (UNISDR 2009). In such cases, the predisposing and triggering factors used in warning and landslide models, the process of disseminating information, the emergency plan, and the educational activities must be considered (Lacasse and Nadim 2009). Therefore, LEWSs need the engagement of scientists, managers and citizens.

In any case, the type, velocity and volume of landslides, the materials involved, the predisposing and triggering factors, and the scale of operation influence the design of the integrated monitoring systems.

In early warning systems for weather-induced landslides, the monitored parameters are classified into three categories: deformation activity (displacements, strains, cracking, micro-seismic and acoustic emissions, rockfall event frequency); groundwater (pore-water pressure, suction, soil humidity); and triggering factors (weather, earthquake, volcanic activity). The monitoring techniques (Safeland 2010, 2012; Guidelines AGI 2023; Dunnicliff 1988; Arattano and Marchi 2008; Casagli et al. 2023; Gupta et al. 2023; Ivanov et al. 2021; Wang et al. 2022; Stähli et al. 2015) include the use of: (i) geodetic methods (global positioning satellite, interferometer, total station); (ii) remote sensing (cameras, ground-based LiDAR, airborne LiDAR, ground-based synthetic aperture radar, interferometric synthetic aperture radar, ground penetrating radar, unmanned aerial vehicles, ground penetrating radar, satellite sensors); (iii) geophysical methods (accelerometers, geophones, time domain reflectometer sensors, electrical conductivity sensors, thermal conductivity sensors); (iv) geotechnical investigations (extensometers, inclinometers, differential monitoring of stability columns, tiltmeters, piezometers, tensiometers, level sensors, contact earth pressure cells, optical fibers, etc.); (v) meteorological instrumentation (rain gauge, snow gauge, weather station).

Deployment of sensor networks provides continuous monitoring, enabling the identification of changes in slope stability.

For debris flow monitoring, parameters such as precipitation, snow depth, water level, negative and positive pore-water pressures, and soil moisture are generally monitored to analyse landslide inception. For the propagation and deposition stages, parameters such as flow depth, flow velocity, and ground vibration are typically considered.

The integrated monitoring system installed in the Favazzina study area was designed both to further validate the methodology proposed by the authors for analysing the inception, propagation and deposition of debris flow, and as part of LEWS.

In previous studies (Ciurleo et al. 2019, 2020, 2021, 2022; Moraci et al. 2017, 2024), debris flow susceptibility maps for the Favazzina site were obtained using the authors' proposed methodology. Based on the best susceptibility map, three monitoring stations were designed and installed in areas identified as most susceptible to debris flow inception (Fig. 3).

Monitoring Station N. 1 (Fig. 4) aims at measuring and recording the triggering and predisposing

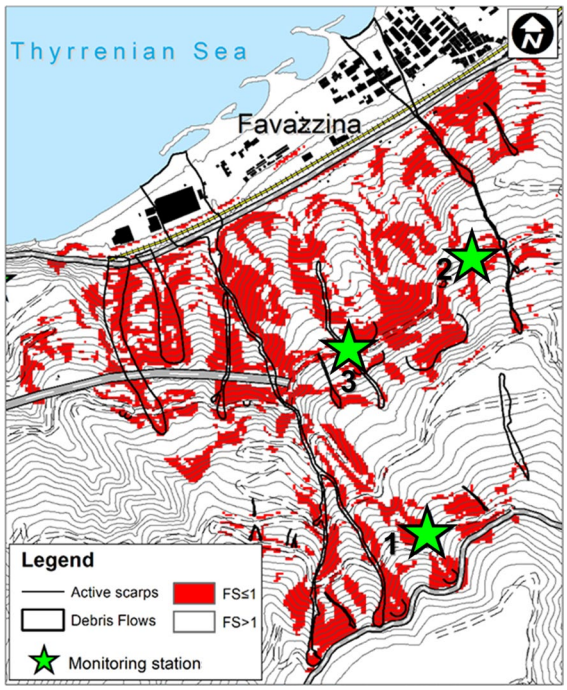

Fig. 3 Best inception susceptibility map used to localize monitoring stations (modified from Ciurleo et al. 2022)

factors of debris flow inception. It is located in the upper zone of the study area and consists of a rain gauge to measure rainfall, coupled with a thermo-hygrometer and a 2D sonic anemometer to measure air humidity and wind speed and direction, respectively. For monitoring predisposing factors, six jet-fill tensiometers for the measurement of negative pore-water pressures, five time domain reflectometer (TDR) sensors, and one capacitive probe for measuring soil water content were installed.

The tensiometers were arranged at various depths (30, 60 × 2, 90, 120 and 150 cm). The capacitive probe allows an almost continuous soil moisture measurement along a 120 cm length and is complemented by the five TDR sensors installed at the same investigation depths as the tensiometers.

In Monitoring Station N. 1, two support poles were installed. One pole supports the rain gauge only, while the other supports the power system, thermo-hygrometer and anemometer. The tensiometers and capacitive probe were installed in the ground between the two poles, and a trench was excavated downstream of the anemometer pole for the TDR sensors. Figure 5 shows the installation scheme of Monitoring Station N.1.

The aim of the two remaining monitoring stations is to measure predisposing factors only. Monitoring Station N. 2, located in the middle zone of the study area (Fig. 6a), consists of five TDR sensors, six jet-fill tensiometers and, one capacitive probe, installed at the same depths as in Monitoring Station N. 1. These instruments, shielded with a PVC platform, were put near the base of an existing retaining wall and connected to an electrical panel mounted on a pole. This station also includes the installation of a piezometer within a core destruction borehole for measuring positive pore-water pressures, and two inclinometers capable of measuring surface layer

Fig. 4 Monitoring Station N. 1

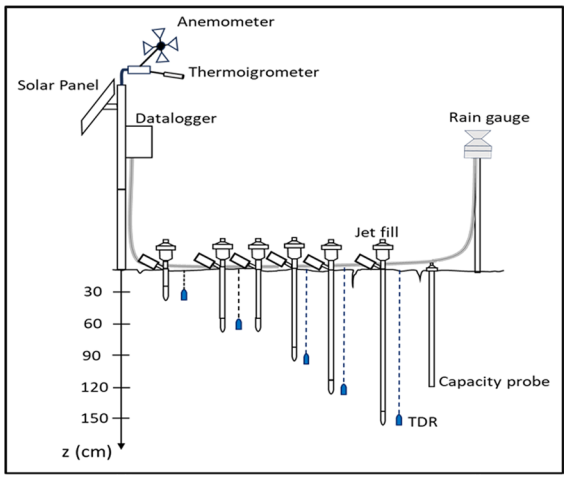

Fig. 5 Installation scheme of Monitoring Station N. 1

displacements, installed within a continuous drilling borehole suitable for both inclinometers.

The first inclinometric column features a 15.5 m long aluminum tube with a 76 mm internal diameter, while the second one features a plastic tube of the same length with a minimum internal diameter of 27 mm. Both tubes were cemented in the same hole.

Monitoring Station N. 3, also located in the middle zone of the study area (Fig. 6b), consists of one piezometer installed within a core destruction borehole and one fixed inclinometer installed within a continuous drilling borehole equipped with a 15.5 m long aluminum tube with an internal diameter of 76 mm.

For monitoring the debris flow propagation stage, six sonic level sensors (SL1 to SL6) and two cameras (CAM1 and CAM2) were installed on cantilever metal structures along the potential path at heights ranging from 2 to 3 m, (Fig. 7). The use of these sensors will provide data on flow depth and flow velocity.

All stations used for inception and propagation analysis are powered by photovoltaic panels (50W) and backup batteries (27AH) connected to a charge controller. They are equipped with data acquisition units and 4G modem routers for data transfer (Fig. 8).

The rain gauge (Fig. 9a) selected for real-time rainfall measurement provides a cumulative measure of precipitation. It is made of UV-stabilized material and is equipped with an internal tipping bucket mechanism that allows for optimal performance

Fig. 6 Monitoring Stations N. 2 (**a**) and N. 3 (**b**)

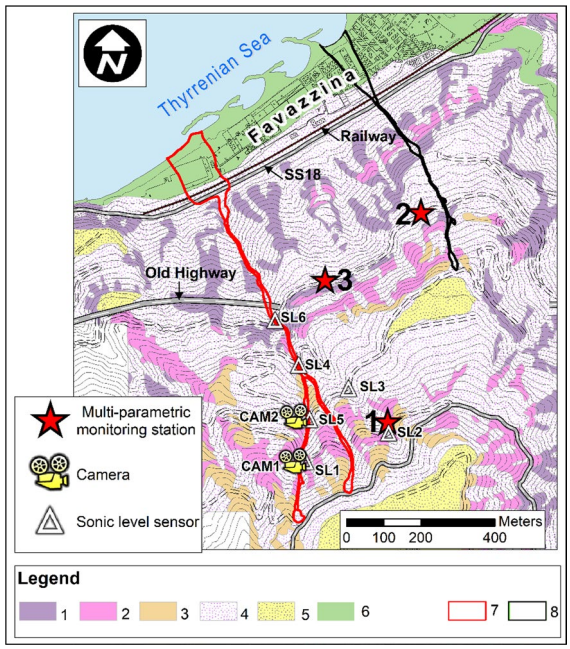

Fig. 7 Monitoring stations and sensors for propagation analysis. Legend: (1) weathered gneiss of class III; (2) weathered gneiss of class IV; (3) weathered gneiss of class V; (4) weathered gneiss of class VI; (5) terraced marine deposits; (6) coastal and alluvial deposits; (7) 2001 debris flow; (8) 2005 debris flow

repeatability. A stainless-steel screen filter channels rainfall, preventing debris from obstructing the flow directed through a nozzle into one of the bucket halves. The tipping mechanism rotates around a pivot and tilts when the first bucket reaches a predetermined level, prompting the second bucket to be positioned under the funnel. When the bucket tips, a reed switch is activated by a magnet attached to the tipping mechanism. The data logger can detect the closure of the reed relay through a pulse channel. The selected rain gauge has an aerodynamic design aimed at preventing air acceleration in its vicinity, thereby ensuring rain remains within the collection container and preserving the measurement's accuracy. Table 1 lists the technical specifications of the selected rain gauge.

For measuring wind speed and direction, a biaxial sonic anemometer was selected (Fig. 9b). This device enables the characterization of wind along two orthogonal axes on the horizontal plane by measuring the time taken for a sound wave to propagate between two pairs of orthogonally oriented transducers comprising the instrument. The transducers bounce the ultrasonic signal from a hood, thus minimizing the effects of transducer shadowing and flow distortion. A characteristic of the chosen anemometer lies in the absence of moving parts, unlike mechanical anemometers, thereby eliminating the need for periodic replacements. The technical specifications of the chosen anemometer are listed in Table 2.

For the measurement of relative humidity and temperature, a thermo-hygrometer was installed (Fig. 9c). This device facilitates the calculation of air pressure and temperature fluctuations, yielding the percentage of humidity present in the air based on the gathered data. It utilizes a single-chip element that integrates both a temperature sensor and a relative humidity sensor, each of them undergoing individual calibration with calibration corrections stored on the chip. A stainless-steel mesh filter minimizes the impact of dust and dirt on the sensor while also facilitating air exchange around the sensor element, thereby reducing the likelihood of condensation remaining inside the filter cap. Additionally, a small PTFE membrane filter is adhered to the surface of the element, preventing any finer dust or mold from directly affecting the measurement. The technical characteristics of the selected thermo-hygrometer are showed in Table 3.

With regard to the measurement of soil volumetric water content, both a preassembled capacitive probe, as well as TDR sensors, were chosen (Fig. 10a, b). The capacitive probe is equipped with 12 sensors spaced at 10 cm intervals and it is tapered, with sensors and electronics encapsulated within the probe plastic using resin; it measures the variation in capacitance between the electrodes inserted into the soil, which are affected by the presence of water content (and hence the apparent dielectric permittivity of the soil). The TDR sensor consists of two 30 cm-long stainless-steel rods connected to the measurement electronics; it calculates the travel time of high-frequency electromagnetic pulses generated and sent along the rods inserted into the soil. When these pulses interact with the water particles present, they are reflected backward toward the sensor. Table 4 lists the technical specifications of both the capacitive probe and the TDR sensors.

For the measurement of negative pore pressures, jet-fill tensiometers (Fig. 11) equipped with five different lengths were installed, coupled with current transducers (specifically, 4-wire, solid-state, differential silicon shear stress/strain gauges). The

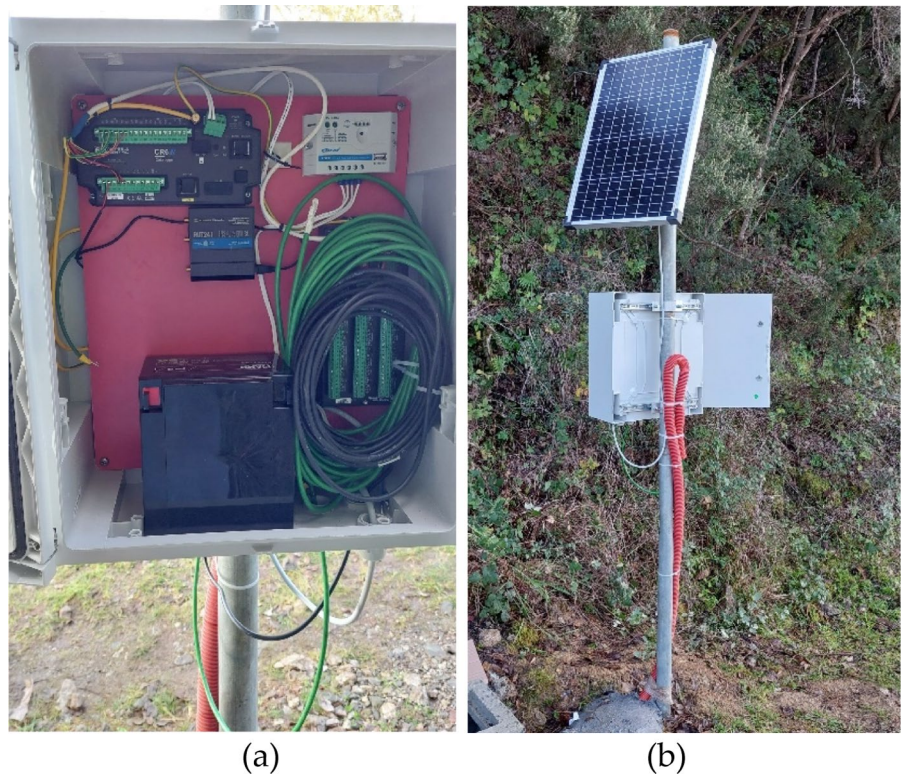

Fig. 8 Data acquisition unit (**a**) and photovoltaic panel (**b**) installed in all monitoring stations

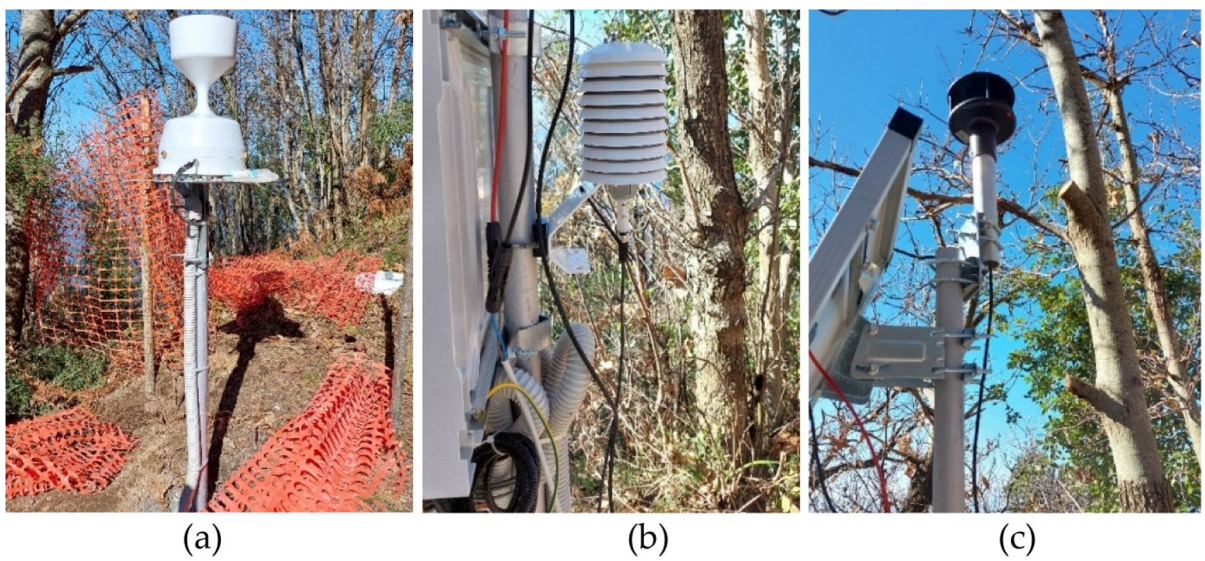

Fig. 9 Rain gauge (**a**), anemometer (**b**) and thermo-hygrometer (**c**) installed in Monitoring Station N. 1

tensiometer consists of a porous ceramic cup, a plastic body tube, and a jet-fill reservoir cap. The ceramic cup is placed in good hydraulic contact with the soil and allows water transfer into and out of the tensiometer body based on the tension (suction) in the soil. The water tension in the soil causes a variation in pressure inside the tensiometer, which can be converted by the current transducer into an electrical

Table 1 Technical specifications for the selected rain gauge

Measure	Rainfall precipitation
Sensor type	Tipping bucket with magnetic reed switch
Rainfall intensity	0–1000 mm/h
Resolution	0.1 mm
Accuracy	±1% up to 120 mm/h
Output	Contact closure (reed switch)
Working temperature	+1 °C/+70 °C
Diameter (funnel)	20 cm
Height	43.5–46.5 cm
Weight	2.5 kg

signal and used to determine the soil suction. The technical characteristics of the coupled tensiometers/current transducers are shown in Table 5.

The selected piezometers are relative electric piezometers designed for measuring water levels in open tubes. They consist of a cylindrical metallic body housing the pressure transducer, complete with a porous front filter made of sintered steel, allowing measurements unaffected by barometric pressure since the sensor membrane communicates with the atmosphere through an integrated compensation capillary tube in the signal cable. The electronic components are fully immersed in resin to ensure long-term sealing. The piezometers were installed with Casagrande cells, positioned as close as possible to the potential sliding surface and equipped with a 12.7 mm diameter tube and a 38.1 mm diameter tube (Fig. 12). Before installing the piezometers, the filters were presaturated. The measurement of interstitial water pressure at the Casagrande cell's installation depth occurs by converting the pressure deforming the membrane connected to the sensor into a proportional electrical signal. The electrical measurement of the output signal in mA is converted into kPa using the instrument's sensitivity value as indicated on the calibration sheet of each instrument. The technical specifications of the chosen piezometers are listed in Table 6.

To monitor ground displacements continuously, chains of fixed inclinometers interconnected by rigid rods and bidirectional joints were installed inside these tubes. Within the inclinometer measuring probes, two digital MEMS (microelectromechanical systems) inclination sensors (biaxial probes) are mounted, measuring the inclination of the probe relative to the vertical in two orthogonal

Table 2 Technical specifications for the selected anemometer

Measure	Wind speed and direction	WIND DIRECTION	
Sensor type	2-dimensional ultrasonic anemometer	Full-scale Range	0°–359°
Measurement frequency	40 Hz block averaged to 1 Hz output frequency	Accuracy	±3°
		Resolution	1°
Working temperature	−35 °C/+70 °C	WIND SPEED	
Diameter	14.2 cm	Full-scale Range	0–60 m/s
Length	16 cm	Accuracy	±2% @ 12 m/s
Weight	0.5 kg	Resolution	0.01 m/s

Table 3 Technical specifications for the selected thermo-hygrometer

Measure	Air temperature and relative humidity	AIR TEMPERATURE	
Sensor type	thermo-hygrometer	Full-scale Range	−40 to +70 °C
Sensor protection	Outer glass-filled PP cap fitted with a stainless steel mesh dust filter with nominal pore size of < 30 µm. The sensor element is fitted with a PTFE protective film with a filtration efficiency of > 99.99% for particles of 200 nm	Accuracy	±0.4 °C
		Resolution	0.001 °C
		RELATIVE HUMIDITY	
		Full-scale Range	0–100% RH
Diameter	12.5 mm	Accuracy	±1.8%@25 °C
Length	115 mm	Resolution	0.001% RH

(a) (b)

Fig. 10 Capacitive probe (**a**) and TDR sensors (**b**) installed in Monitoring Station N. 1

Table 4 Technical specifications for capacitive probe and TDR sensors

Measure	Volumetric water content	
Sensor type	Capacitive probe	TDR sensor
Range	0% to saturation	0% to saturation
Resolution	1:10,000	0.1% VWC
Precision	±0.03% vol	Better than 0.1% VWC
Working temperature	−20 °C/+60 °C	0 °C/+70 °C
Probe dimensions	Diameter: 24.5 mm	Head: 85×63×18 mm

Fig. 11 Tensiometers installed in Monitoring Station N. 1

planes passing through the probes axis. Specifically, at the Monitoring Station N. 2, a 15 m long digital inclinometer chain (Fig. 13a) with 25 sensor nodes was installed; it is constructed with 5 modular segments of 3 m, with independent rods made of highly durable metallic material with a 0.61 m pitch connected by mechanical joints, each equipped with a biaxial inclinometer sensor. Close to it, a 15 m long digital inclinometer chain (Fig. 13b) with 30 instrumented nodes equipped with biaxial inclinometer

Table 5 Technical specifications for coupled tensiometers/current transducers

Measure	Negative pore water pressure
Sensor type	Jet-fill tensiometer and solid state differential silicon shear stress/strain gauge
Full-scale range	0–1 bar
Linearity	0.25% F.S
Output	4–20 mA
Working Temperature	0 °C/+ 60 °C
Tensiometer length	30, 60, 90, 120, 150 cm

Fig. 12 Piezometer installed in Monitoring Station N. 2

Table 6 Technical specifications for the selected piezometers

Measure	Positive pore water pressure
Sensor type	Relative piezometer
Full-scale range	200 kPa
Sensitivity	0.01% F.S
Accuracy	0.3% F.S
Output	4–20 mA
Working Temperature	− 10 °C/+ 70 °C
Diameter	22 mm
Length	190 mm
Weight	0.25 kg

sensors with a 0.5 m pitch, constructed with rigid segments, preassembled with flexible joints, and protected by a double layer of stainless-steel braid was installed as well. Figure 13c shows the installation phase of both the inclinometer chains.

At Monitoring Station N. 3, a 13 m long digital inclinometer chain (Fig. 14) was installed, consisting of seven probes, five of which are 2 m long (1.5 m carbon fiber rod) and two are 1.5 m long (1 m rod), equipped with biaxial sensors in stainless steel casings. The technical specifications of the chosen inclinometer chains are listed in Table 7.

All monitoring points containing piezometers and inclinometers feature a protective pit equipped with a cover positioned over the head of the tubes to accommodate instrument anchoring material and cable passage. In Monitoring Stations N.2 and N.3, the two instrument boreholes are connected at the head via corrugated conduits, with an internal diameter of 4 cm, which extend from the boreholes along a 3-m pole up to a height of 1.80 m from the ground level, providing protection for four multipolar cables. The 3-m pole allows for the installation of the reference data acquisition unit and the photovoltaic panel.

To capture and record the debris flow phenomenon, compact cameras with a 4 K UHD resolution image sensor at a frequency of 30 frames per second were installed (Fig. 15a). These cameras have a horizontal image angle of 45°, an integrated temperature sensor, an audio module (microphone and speaker), and an 8 GB micro SD internal DVR. They are housed in cases with an IP66 protection rating and utilize applications supported by artificial intelligence and deep learning. The entire video analysis and recording occur within the camera in real-time and with an integrated video processing. Images are captured in color during the day and in black and white at night. Table 8 lists the technical specifications of the chosen cameras.

In this research, sonic ranging sensors designed for a non-contact assessment of debris flow depth were installed (Fig. 15b). These sensors gauge depth by emitting an ultrasonic pulse (50 kHz), which is reflected back when encountering a reflective object (such as debris flows) and captured by the sensor. The time taken for the sound waves reflected from the target to return is measured. Given the well-established variable of the speed of sound, the distance to the

Fig. 13 Inclinometers installed in Monitoring Station N. 2: 25 sensor nodes inclinometer (**a**), 30 sensor nodes inclinometer (**b**), and installation phase (**c**)

object can be determined. Table 9 lists the technical specifications of the chosen sonic ranging sensors.

4 Discussion and Conclusions

The main objective of designing this monitoring system is to validate existing and potential landslide inception and propagation models used in previous research. This validation aims to fine-tune the landslide inception model and the alert model for using it in early warning systems, after a sufficiently extensive monitoring period.

The design of the integrated monitoring system, the definition of the acquisition time and the processing of the measured data were based on previous studies conducted in the study area. The best susceptibility map obtained by the authors (Fig. 3) was used to locate the three monitoring stations aimed at validating and forecasting the proposed inception methodology,.

Geophysical investigations, consisting of twenty-six seismic refraction tomographies (each 48 m long), and in situ geotechnical investigations, comprising eighteen mechanical continuous borehole drilling with depths ranging from 5 to 20 m, allowed identifying the thickness of the class VI gneiss (about 2 m at the head of channels). This made it possible to determine the depths at which instruments (tensiometers, TDR sensors and capacitive probes) were installed in Monitoring Stations N.1 and 2 (Fig. 16). Additionally, two piezometers were installed at the base of class VI gneiss at depths of 1.70 m and 2.0 m in Monitoring Stations N.2 and N.3, respectively. The maximum soil depth for embedding inclinometer casing tubes was also defined using the same investigations.

Instrumentation for monitoring the propagation phase (cameras and sonic ranging sensors) was located along the propagation path of significant past debris flows in the study area (2001 and 2005). Numerical analyses of these events provided data on the height and velocity of the debris flow front, which made it possible to set both the height for the sonic

Fig. 14 Inclinometer installed in Monitoring Station N. 3

Table 7 Technical specifications for inclinometers

Measure	Horizontal displacement		
Sensor type	MEMS sensor	MEMS sensor	MEMS sensor
Range	±30°	±60°	±15°
Resolution	9 arcseconds	±2 arcseconds	0.00056°
Working Temperature	− 10 °C/+ 40 °C	− 35 °C/+ 60 °C	− 30 °C/+ 70 °C
Weight	0.54 kg per 0.6 m gauge length	0.2 kg/segment	2.4 kg in total (1.5 m length)/2.5 kg in total (2 m length)

ranging sensors (Fig. 17) and the optimal distance between different sensors, necessary to optimize their acquisition time.

The decision to use multiple instruments measuring the same parameters, such as TDR sensors and capacitive probes, or two types of inclinometers in the same borehole, was driven by the intention to design a redundant monitoring system, thereby increasing system reliability. Redundant sensors allow the system to continue functioning despite individual component failures without compromising overall performance. Additionally, this setup aims at verifying, for research purposes, the accuracy of conventional instruments compared to more advanced ones. Furthermore, both the capacitive probe and the TDR sensors were selected and positioned within the soil to ensure nearly continuous soil moisture measurement along the depth of investigation. Similarly, TDR sensor installation depths matched those of the jet-fill tensiometers to correlate in situ soil water content with negative pore-water pressures measured at the same depths. The decision to use fixed inclinometers, despite providing less detailed deformation profiles than manual probes, was driven by the fact that, in the monitored phenomenon, displacements are concentrated in shallow depth layers. Additionally, these

Fig. 15 Monitoring stations for debris flow propagation: camera (**a**); sonic ranging sensor (**b**) and Monitoring Station Cam 1—SL1 (**c**)

Table 8 Technical specifications for the selected cameras

Measure	Flow motion
Resolution	4 K UHD
Max frame rate	(MxPEG+): 20fps@4 K
Chip	Quad-core ARM Cortex-A53 (up to 1300 MHz)
Accuracy	± 1 cm or 0.4% of distance to target, whichever is greater
Working Temperature	− 40 °C/+ 65 °C

Table 9 Technical specifications for the selected sonic ranging sensors

Measure	Debris flow depth
Sensor type	sonic
Range	0.5–10 m
Resolution	0.25 mm
Accuracy	± 1 cm or 0.4% of distance to target, whichever is greater
Working Temperature	− 45 °C/+ 50 °C
Diameter	7.6 cm
Length	10.1 cm
Weight	0.4 kg

movements are analysed alongside other variables, such as pore-water pressures, whose variations occur so rapidly that they require high-frequency measurements not feasible with manual readings conducted with removable inclinometers.

Moreover, landslide monitoring systems rely on electrical power sources, such as batteries and solar panels, ensuring power redundancy. The reason to implement redundant power supplies is to ensure continuous operation even if the primary power source fails or is disrupted.

Finally, the temporal frequency for instrument data acquisition for inception analysis was selected to also develop a potential warning model for early warning systems. Continuous and real-time rainfall data acquisition is essential,, hence the chosen temporal frequency values. For other sensors (jet-fill tensiometers, TDR sensors and capacitive probe), a precautionary data acquisition frequency of 30 s was set, considering the shallower sensors, soil hydraulic conductivity, state parameters, and potential drying vertical cracks.

Additionally, the temporal frequency for data acquisition of the instruments installed for the propagation analysis was set considering both the numerical analysis results and the instrumentation features. Specifically, the decision to capture images at a

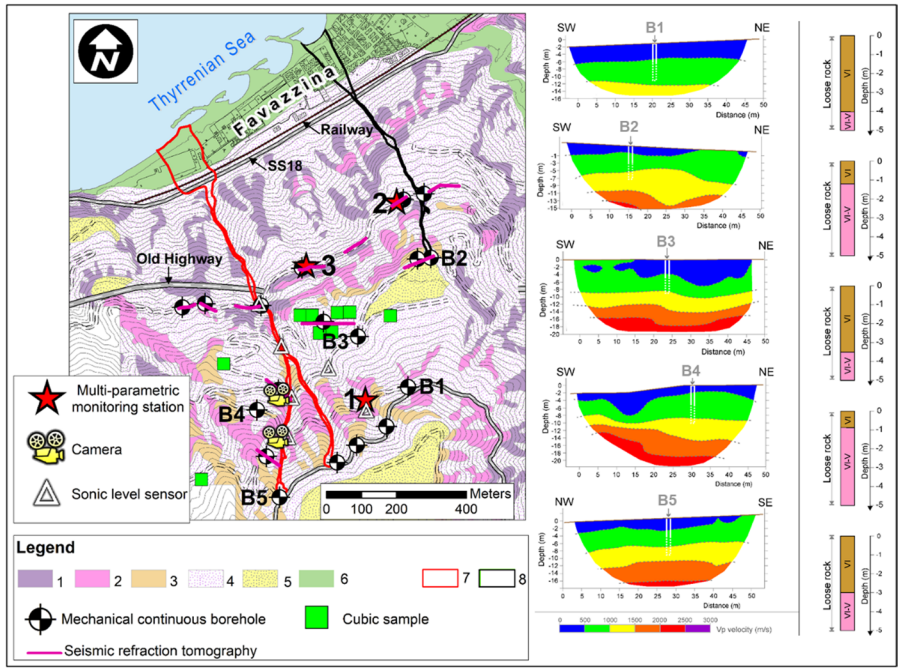

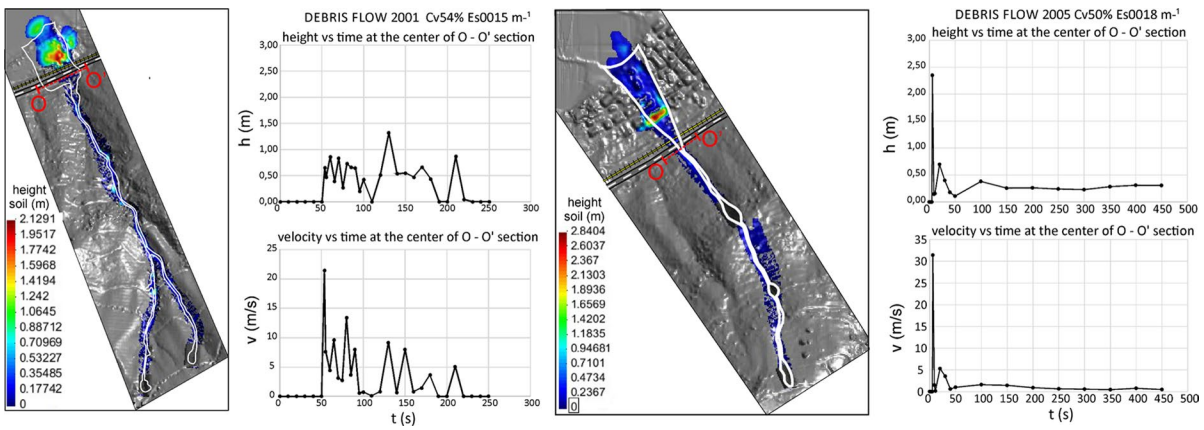

Fig. 16 Geophysical and geotechnical in situ investigations (modified from Ciurleo et al. 2020). Legend: (1) weathered gneiss of class III; (2) weathered gneiss of class IV; (3) weathered gneiss of class V; (4) weathered gneiss of class VI; (5) terraced marine deposits; (6) coastal and alluvial deposits; (7) 2001 debris flow; (8) 2005 debris flow

Fig. 17 Propagation analysis results for the most significant debris flows occurred in the study area (modified from Ciurleo et al. 2020)

frequency of 30 frames per second was influenced by the potential use of these images for particle tracking velocimetry (tracking the movement of individual particles) or particle image velocimetry (measuring the average displacement of a set of particles). Since determining flow velocity with these techniques involves dividing particle movement between two consecutive frames by the time interval for capturing image pairs, setting the correct values for spatial and temporal resolution is essential. Regarding the sonic ranging sensors, the temporal frequency for data acquisition was set to one second considering the flow velocity, the minimum distance between two sensors, and their measurement time.

The use of instruments like piezometers, inclinometers, tensiometers, TDR sensors and capacitive probes, installed within slopes susceptible to debris flow inception, can be extremely useful to complement rainfall measures. These instruments make it possible to quantify the effect of rainfall on the

water advance front inside the soils involved in the shallow landslides (class VI gneiss), consequently changing soil suction and shear strength, and on the groundwater. This will help improve the landslide inception and warning models. On the other hand, instruments such as cameras and sonic ranging sensors used to monitor debris flow propagation help refine the landslide propagation model, enabling the design of risk mitigation protective measures.

Therefore, the novelty of this study lies in the methodological approach used to design the integrated monitoring system, starting from the best susceptibility map for the inception of the area obtained by the authors in previous studies. The monitoring system, founded on traditional and innovative technologies, can be used both to validate the integrated methodology proposed by the authors for analysing the inception, propagation, and accumulation of debris flows and to define the alert model for using it in early warning systems for fast landslides. Once the methodological approach is validated at an intermediate scale and verified by the in situ integrated monitoring system descibed in this paper, it can be trasferred to different scales in similar geological and geotechinal contexts. Therefore, the proposed methodology, coupled with the integrated monitoring system, could become a relevant tool for the management and the mitigation of landslide risk at both local and territorial scale.

Author Contributions Conceptualization, all authors; formal analysis, all authors; investigation, all authors; data curation, all authors; writing—original draft preparation, all authors; writing—review and editing, all authors; visualization, all authors; supervision, Nicola Moraci; project administration, Nicola Moraci; funding acquisition, Nicola Moraci. All authors have read and agreed to the published version of the manuscript.

Funding Open access funding provided by Università degli Studi Mediterranea di Reggio Calabria within the CRUI-CARE Agreement. This work was partially funded by the Next Generation EU—Italian NRRP, Mission 4, Component 2, Investment 1.5, call for the creation and strengthening of 'Innovation Ecosystems', building 'Territorial R&D Leaders' (Directorial Decree n. 2021/3277)—project Tech4You—Technologies for climate change adaptation and quality of life improvement, n. ECS0000009. The research was also partially supported by the European Union—FSE—REACT—EU, PON Research and Innovation 2014–2020, DM1062/2021, CCI2014IT-16M2OP005 (CUP C35F21001220009 code: I06). This work reflects only the authors' views and opinions, neither the Ministry for University and Research nor the European Commission can be considered responsible for them.

Data Availability Data generated or analyzed during this study are available from the corresponding author upon reasonable request.

Declarations

Conflict of interest The authors declare that they have no competing interests.

References

Arattano M, Marchi L (2008) Systems and sensors for debris-flow monitoring and warning. Sensors 8:2436–2452

Baum RL, Savage WZ, Godt JW (2002) TRIGRS-A Fortran program for transient rainfall infiltration and grid-based regional slope-stability analysis. US Geological Survey, Open-File Report 02-0424

Biondino D, Borrelli L, Critelli S, Muto F, Apollaro C, Coniglio S, Tripodi V, Perri F (2020) A multidisciplinary approach to investigate weathering processes affecting gneissic rocks (Calabria, southern Italy). CATENA 187:104372

Calvello M (2017) Early warning strategies to cope with landslide risk. Riv Ital Geotec 2:63–91

Casagli N, Intrieri E, Tofani V, Gigli G, Raspini F (2023) Landslide detection, monitoring and prediction with remote-sensing techniques. Nat Rev Earth Environ 4:51–64

Ciurleo M, Mandaglio MC, Moraci N (2019) Landslide susceptibility assessment by TRIGRS in a frequently affected shallow instability area. Landslides 16:175–188

Ciurleo M, Mandaglio MC, Moraci N, Pitasi A (2020) A method to evaluate debris flow triggering and propagation by numerical analyses. Lect Notes Civ Eng 40:33–41

Ciurleo M, Mandaglio MC, Moraci N (2021) A quantitative approach for debris flow inception and propagation analysis in the lead up to risk management. Landslides 18:2073–2093

Ciurleo M, Ferlisi S, Foresta V, Mandaglio MC, Moraci N (2022) Landslide susceptibility analysis by applying

TRIGRS to a reliable geotechnical slope model. Geosciences 12(18):13
Corominas J, van Westen C, Frattini P, Cascini L, Malet JP, Fotopoulou S, Catani F, Van Den Eeckhaut M, Mavrouli O, Agliardi F, Pitilakis K, Winter MG, Pastor M, Ferlisi S, Tofani V, Hervás J, Smith JT (2014) Recommendations for the quantitative analysis of landslide risk. Bull Eng Geol Environ 73:209–263
Dunnicliff J (1988) Geotechnical instrumentation for monitoring field performance. Wiley, p 577
Fell R, Ho KKS, Lacasse S, Leroi E (2005) A framework for landslide risk assessment and management. Landslide Risk Manag 13–36
Fell R, Corominas J, Bonnard C, Cascini L, Leroi E, Savage WZ, On behalf of the JTC-1 Joint Technical Committee on Landslides and Engineered Slopes (2008) Guidelines for landslide susceptibility, hazard and risk zoning for land-use planning. Eng Geol 102:85–98
Gioffrè D, Mandaglio MC, Ciurleo M, Moraci N (2023) Deformative response of sheltering structures under the debris flow impact. Int J Geosynth Ground Eng 9(6):70
Guidelines AGI-ISPRA (2022) Progettazione degli Interventi di Mitigazione del Rischio da Frana. AGI, Roma, p 107
Guidelines AGI (2023) Raccomandazioni sul monitoraggio geotecnico—misure inclinometriche. AGI, Roma, p 75
Gupta B, Sharma K, Koirala T, Sharma S (2023) IoT-based landslide monitoring system using LiDAR sensors: a review. Part of the lecture notes in networks and systems book series. LNNS, vol 535
Ivanov V, Longoni L, Ferrario M, Brunero M, Arosio D, Papini M (2021) Applicability of an interferometric optical fibre sensor for shallow landslide monitoring—experimental tests. Eng Geol 288:106128
Lacasse S, Nadim F (2009) Landslide risk assessment and mitigation strategy. In: Sassa K, Canuti P (eds) Landslides—disaster risk reduction. Springer, Berlin, Heidelberg, pp 31–61
Moraci N, Mandaglio MC, Gioffrè D, Pitasi A (2017) Debris flow susceptibility zoning: an approach applied to a study area. Riv Ital Geotec 51:47–62
Moraci N, Mandaglio MC, Ciurleo M (2024) A three stage method for debris flow analysis. In: Hazarika H, Haigh SK, Chaudhary B, Murai M, Manandhar S (eds) Sustainable construction resources in geotechnical engineering, select proceedings of the 2nd international conference on construction resources for environmentally sustainable technologies (CREST 2023). Springer, Singapore. eBook ISBN 978-981-99-9227-0
Pastor M, Haddad B, Sorbino G, Cuomo S, Drempetic V (2009) A depth integrated coupled SPH model for flow-like landslides and related phenomena. Int J Numer Anal Methods Geomech 33(2):143–172
Pecoraro G, Calvello M, Piciullo L (2019) Monitoring strategies for local landslide early warning systems. Landslides 16:213–231
Safeland (2010) Deliverable D4.1 "Review of techniques for landslide detection, fast characterization, rapid mapping and long-term monitoring". In: Michoud C, Abellán A, Derron MH, Jaboyedoff M (eds), Grant Agreement n. 226479, p 401
Safeland (2012) Deliverable D4.8 "Guidelines for landslide monitoring and early warning systems in Europe—design and required technology" In: Bazin S (ed), Grant Agreement n. 226479, p 153
Stähli M, Sättele M, Huggel C, Mcardell BW, Lehmann P, Van Herwijnen A, Berne A, Schleiss M, Ferrari A, Kos A, Or D, Springman SM (2015) Monitoring and prediction in early warning systems for rapid mass movements. Nat Hazards Earth Syst Sci 15(4):905–917
UNISDR (2009) Terminology on disaster risk reduction. https://www.undrr.org/publication/-unisdr-terminology-disdisaster-risk-reduction
Wang C, Guo W, Yang K, Wang X, Meng Q (2022) Real-time monitoring system of landslide based on LoRa architecture. Front Earth Sci 10:899509